Long-term morphological developments of river channels separated by a longitudinal training wall

Le, Binh; Crosato, Alessandra; Uijttewaal, Wim

DOI
10.1016/j.advwatres.2018.01.007

Publication date
2018

Document Version
Final published version

Published in
Advances in Water Resources

Advances in Water Resources 113 (2018) 73–85

Contents lists available at ScienceDirect

Advances in Water Resources

journal homepage: www.elsevier.com/locate/advwatres

Long-term morphological developments of river channels separated by a longitudinal training wall

T.B. Le[a,b,*], A. Crosato[a,c], W.S.J. Uijttewaal[a]

[a] Delft University of Technology, PO Box 5048, Delft 2600, GA, The Netherlands
[b] Thuy Loi University, 175 Tay Son, Dong Da, Hanoi, Vietnam
[c] IHE Delft, Department of Water Engineering, PO Box 3015, Delft 2601, GA, The Netherlands

ARTICLE INFO

Keywords:
Longitudinal training wall
River morphology
River bars
Channel stability
Delft3D
Laboratory experiments

ABSTRACT

Rivers have been trained for centuries by channel narrowing and straightening. This caused important damages to their ecosystems, particularly around the bank areas. We analyze here the possibility to train rivers in a new way by subdividing their channel in main and ecological channel with a longitudinal training wall. The effectiveness of longitudinal training walls in achieving this goal and their long-term effects on the river morphology have not been thoroughly investigated yet. In particular, studies that assess the stability of the two parallel channels separated by the training wall are still lacking. This work studies the long-term morphological developments of river channels subdivided by a longitudinal training wall in the presence of steady alternate bars. This type of bars, common in alluvial rivers, alters the flow field and the sediment transport direction and might affect the stability of the bifurcating system. The work comprises both laboratory experiments and numerical simulations (Delft3D). The results show that a system of parallel channels divided by a longitudinal training wall has the tendency to become unstable. An important factor is found to be the location of the upstream termination of the longitudinal wall with respect to a neighboring steady bar. The relative widths of the two parallel channels separated by the wall and variable discharge do not substantially change the final evolution of the system.

1. Introduction

Many low-land rivers are used for inland navigation, as for instance the Waal (de Vriend, 2015), the Elbe (Elbe Promotion Centre, website), the Thames (British Marine Federation and Environment Agency, 2013), the Mississippi (Army Corps of Engineers, 2011). Important plans to improve inland navigation regard the White Nile and Nile Rivers in Sudan (NEPAD Agency, 2013) as well as the Me Kong River in Vietnam (Mekong River Commission, 2016), among others. These rivers still present long reaches with natural banks and new interventions should be planned in a way to preserve their most important ecological aspects. For this reason, it is important to study new training techniques that allow for the co-existence of navigation with natural banks, without affecting flood water levels.

The creation of a navigation route often includes channel narrowing. This results in a deeper river channel and reduces bar formation (Duró et al., 2015), which is good for navigation. River are narrowed by constructing series of groynes along both sides of the river, as in the Rhine (Havinga et al., 2006) and Rhone Rivers (Scerri et al., 2015), or by bank protection works, especially in urban areas. As a result, bed degradation occurs in the narrowed reach and upstream. In the narrowed reach, the water depth increases; upstream, the water depth tends to remain the same as before the intervention, but both bed and water levels decrease, as shown by Jansen et al. (1979). Bed degradation is amplified by river shortening, another frequent intervention aiming at navigation improvement (e.g. Spinewine and Zech, 2008). Moreover, maintaining the navigation channel during low-flow conditions, when bars and other sediment deposits obstruct the navigation route often requires dredging, which is in some cases accompanied by dumping of dredged sediment in deep areas (Mosselman et al., 2004; Sieben, 2009; van Vuren et al., 2015). Without dumping, sediment extraction results in important incision processes along the entire river course, strengthening the effects of the other interventions aimed at navigation route improvement, such as channel narrowing and shortening (e.g. Visser et al., 1999; de Vriend, 2015). Bed and water level degradation affect intakes and the foundations of structures along the river, including the groynes, and lower groundwater levels, with consequences for floodplain vegetation and agriculture in the area adjacent to the river. Excessive bed degradation can even cause problems to navigation if rock outcrops appear, as along the Rhine River between

* Corresponding author.
E-mail address: T.B.Le@tudelft.nl (T.B. Le).

https://doi.org/10.1016/j.advwatres.2018.01.007
Received 31 May 2017; Received in revised form 12 December 2017; Accepted 7 January 2018
Available online 09 January 2018

Cologne and Rees (Frings et al., 2014).

Another problem related to traditional river training is that banks protected by groynes or by revetments lose their natural value. This can be observed in many trained rivers, for which the restoration of the riverine environment has become a priority (e.g. Schoor et al., 1999). However, at the same time, the restored river should have similar or even increased high-flow conveyance (e.g. Villada Arroyave and Crosato, 2010) to reduce the probability of floods along its course. All these issues show the need to define new, more sustainable, river management strategies (Rijke et al., 2012).

In this paper, we study the possibility of obtaining a stable navigation channel minimizing river ecosystem degradation, without affecting flood water levels. The idea is to create two parallel channels, one for navigation and one for ecology, which may have the same width or different widths, by means of a longitudinal wall. The system of parallel channels separated by a longitudinal wall starts with an upstream bifurcation. Previous work has shown that the stability of bifurcating channels depends on the distribution of flow and sediment at the bifurcation point (Flokstra, 1985): if one branch receives more sediment than the flow can transport, it gradually silts up; instead, if it receives less sediment than its transport capacity its bed is eroded. In the latter case, with the progression of bed erosion the branch receives increasing amounts of water, which intensifies the erosion process (Wang et al., 1995) and at the same time increases deposition in the other branch. Unbalanced sediment inputs therefore lead to the instability of the system.

This work focuses on the long-term stability of the two channels separated by a longitudinal wall in rivers with steady or slowly migrating alternate bars. These bars are common features in alluvial rivers (Fig. 1). Steady bars in the river channel close to the bifurcation point permanently alter both the water flow pattern and the sediment transport direction. Therefore, bars are expected to affect the sediment distribution between the two channels, with possible consequences for their stability (Sloff and Mosselman, 2012, and Redolfi et al., 2016).

The work includes laboratory and numerical investigations. The laboratory investigation analyses the morphological evolution of a straight channel with steady alternate bars divided by a longitudinal wall. Different width ratios and locations of the starting point of the structure with respect to one bar are considered, with the aim to define the conditions for obtaining a stable system. The numerical investigation, carried out using the open-source Delft3D code, analyses the applicability of the technology to real river cases. First, the most significant flume test is upscaled and simulated to establish whether the numerical model is able to reproduce the processes observed in the laboratory, but this time considering a similar system having a real river size. Then, the code is applied to the Alpine Rhine River (Adami et al., 2016), a natural system that is rather similar to the upscaled one and presents regular alternate bars with low migration rates. This part of the study focuses on the effects of variable discharge on the stability of the two-channel system, on bar formation inside the bifurcating channels and on flow conveyance. The work does not include any constructive issues (presence of openings, wall top level, etc.) that may influence the channel morphological changes and therefore the stability of the system.

2. River bars and bifurcations

River bars are large sediment deposits that become visible during low flows surrounded by deep areas (pools). Bars can be classified in three main categories: forced, free and hybrid (Duró et al., 2015). *Forced bars* are local deposits that form due to persistent flow pattern imposed by the channel geometry or by external factors (forcing). A typical example of forced bars is the point bars inside river bends. *Free bars* are large bed undulations that form due an instability phenomenon of alluvial river beds (Hansen, 1967; Callander, 1969; Tubino et al., 1999) having a wavelength that compares with the channel width and amplitude that compares with the water depth. Their number in the river cross-section is represented by the "mode", m (Engelund, 1970). This is the integer of the ratio between the transverse half-wavelength of the bars that form in the channel and the channel width: $m = 1$ corresponds to a series of bars that alternately form near one side and then the other (alternate bars), typical of meandering rivers; $m = 2$ to central bars; and $m > 2$ to multiple bars. Modes larger than two correspond to a multiple-thread channel with more than one bar in the cross-section, typical of braided rivers (Fredsøe, 1978; Parker, 1976; Crosato and Mosselman, 2009). Free bars normally migrate either in upstream or downstream direction (Zolezzi and Seminara, 2001). The mode and the other bar characteristics, such as wave length, amplitude, migration celerity and growth rate depend on flow width-to-depth ratio, Shield number and other morphodynamic parameters (e.g. Tubino and Seminara, 1990). In particular, bars form only if the width-to-depth ratio exceeds a critical value and this critical value is larger for larger bar modes (Engelund, 1970). *Hybrid bars* are non-migrating bars similar to free bars. Their existence is due to the interaction of forcing and morphodynamic instability. Persistent geometric discontinuities of the channel (asymmetric narrowing, widening, and structures), which are rather common in rivers, act as forcing: they fix the location of the bars and impose to them zero celerity and a corresponding wavelength. The wavelength of hybrid alternate bars is generally 2–3 times longer than the wavelength of alternate free bars.

The effects of free migrating bars on bifurcations were studied by Bertoldi et al. (2009). Migrating bars arrive at the bifurcation alternatively on one side and then the other. They feed the downstream branches alternatively with a larger and then smaller amount of water and sediment. As a result, the bifurcation oscillates around an equilibrium or disappears due to closure of one of the branches.

Steady bars permanently affect the sediment transport distribution between the two branches of a bifurcation (Redolfi et al., 2016). This is due to the combination of flow deformation and gravity. Due to the presence of bars, the flow follows a weakly meandering pattern and concentrates in the pools. For this, the branch closest to the pool receives most discharge and most sediment. Gravity alters the direction of bed material moving on bar slopes deviating sediment towards the pool (Talmon et al., 1995). Finally, bars impose a certain curvature to the stream lines, producing a (weak) spiral flow that deflects the sediment moving near the bed, this time towards the bar tops (Struiksma et al., 1985). The effects of bars on bifurcation stability depends on the interaction between these phenomena.

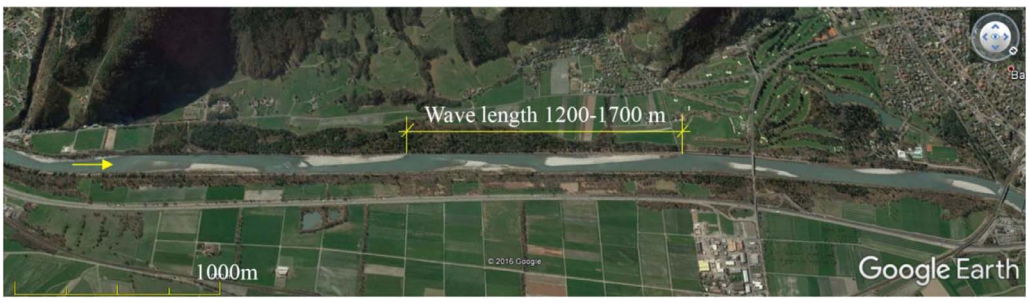

Fig. 1. Bars migrate slowly and after 26 year they are more or less at the same location in the Alpine Rhine River between Landquart and Bad Ragaz, Switzerland (Adami et al., 2016)(Google Earth © 2016).

Considering that water depth, channel width and other variables depend on flow characteristics, it can be expected that bars change shape and migration celerity due to discharge variations. This was investigated by Tubino (1991) on free bars, but works studying the effects of varying discharge on the characteristics of hybrid and forced bars are lacking. It is likely that also this type of bars changes geometry as a result of flow alterations, although to a lesser extent than free bars, because the effects of discharge are mitigated by the presence of the forcing. However, also the effect of geometrical discontinuities depends on discharge. This means that we can expect point bar and hybrid bar elongation or shortening due to the increase or decrease of flow discharge. This might mean that bars may affect the distribution of sediment and water between bifurcating channels in a different way depending on discharge and thus the hydrograph.

The morphological evolution of each branch of a bifurcation includes gradual changes of mode and other bar characteristics, as a direct consequence of bed elevation and water depth changes. We can generally expect bed degradation to contribute to gradual bar suppression (decreasing width-to-depth ratio) and bed aggradation to the opposite.

3. Methodology

The method adopted in this study includes both experimental and numerical investigations. The experiments were carried out at the Laboratory of Fluid Mechanics of Delft University of Technology in a 14.4 m long and 0.4 m wide straight flume with a sandy bed presenting steady or slowly migrating alternate bars. The longitudinal training wall was reproduced by a thin longitudinal plate which subdivided the original channel in two parallel channels, the bifurcation point being the location of the upstream termination of this plate. Considering that the water and sediment distribution between the parallel channels may depend on the location of the bifurcation with respect to a neighboring steady bar, for every experiment two different locations were tested: one at the upstream part of a bar and the other one at the downstream part, in the pool area. Different subdivisions were studied to assess the role of relative channel width on the developments (timing and system stability): B_e: B_n = 1:5, 1:3 and 1:1, being B_e and B_n the widths of the two branches of the bifurcation, here named the “ecological” and the “navigation” channel, respectively. The last one corresponds to a subdivision in two parallel channels having the same width. Additionally, extra tests were carried out using different sands to compare to the response of systems with different degrees of sediment suspension, also considering that the effects of transverse bed slope on sediment transport are relatively less important for small sediment sizes than for larger sediment sizes (Chavarrías et al., 2013).

The formula by Crosato and Mosselman (2009) was used for the preliminary selection of the morphodynamic characteristics of the laboratory stream. The formula allows deriving the mode m of hybrid bars that form in the channel. The formation of hybrid alternate bars is expected if the chosen combination of parameters results in $m = 1$:

$$m^2 = 0,\ 17g\frac{(b-3)}{\sqrt{\Delta D_{50}}}\frac{B^3 i}{CQ} \tag{1}$$

where m is the bar mode, g is the gravity acceleration, b is the degree of non-linearity of the sediment transport formula as a function of flow velocity, B is the channel width, i is the longitudinal bed slope, Δ is the relative submerged sediment density, D_{50} is the median sediment size, C is the Chézy coefficient and Q is the discharge.

To allow observing the alternate bars in the 14 m long flume, the bar wavelength should not be too long. Ideally, 2–3 bars should be present in the channel. To check this, the theoretical hybrid bar wavelength was computed using the following equation (Struiksma et al., 1985):

$$\frac{2\pi}{L_p} = \frac{1}{2\lambda_W}\left[(b+1)\frac{\lambda_W}{\lambda_S} - \left(\frac{\lambda_W}{\lambda_S}\right)^2 - \frac{(b-3)^2}{4}\right]^{1/2} \tag{2}$$

where L_p is the hybrid bar wavelength, λ_w is the 2D flow adaptation length, λ_s is the 2D water depth adaptation length.

$$\lambda_W = \frac{h_0}{2C_f} \tag{3}$$

$$\lambda_S = \frac{1}{(m\pi)^2} h_0 \left(\frac{B}{h_0}\right)^2 f(\theta_0) \tag{4}$$

in which h_0 is the normal depth, C_f is the friction factor defined by $C_f = \frac{g}{C^2}$, $f(\theta_0)$ accounts for the effect of gravity on the direction of sediment transport over transverse bed slopes. It is calculated as Talmon et al. (1995)

$$f(\theta_0) = \frac{0.85}{E}\sqrt{\theta_0} \tag{5}$$

where E is a calibration coefficient and θ_0 is the Shields parameter.

The ratio $\alpha = \lambda_S/\lambda_W$ is called “interaction parameter” and is a characteristic of the 2D response of an alluvial channel (Struiksma et al., 1985).

Eq. (2) was derived from a linear model and for this the value of L_p provides only a rough estimate of the wavelength of the bars in the final stages of their development. Nevertheless, the formula has been observed to function rather well on experimental settings (Struiksma and Crosato, 1989). Eq. (2) was applied in this study to check the experimental settings with the aim to obtain 2 to 3 bars in the flume.

Bars are expected to alter the subdivision of sediment between the parallel channels in a different way, depending on sediment transport mechanism and on transverse bed slope alteration of sediment transport direction. Considering that both mechanisms depend on sediment size, the laboratory investigation includes four extra tests with two different sands (sensitivity analysis).

The numerical simulations consisted of two investigations: the first one was meant to assess the capability of the numerical model to reproduce the morphological processes observed in the laboratory; the other one was an application of the model to a real river case. The first model application simulated the morphological evolution observed in the base-case laboratory scenario and consisted of two runs. This was done on an upscaled numerical version of the experiments having the same longitudinal bed slope, Shields parameter, width-to-depth ratio, bar mode and 2D interaction parameter (Kleinhans et al., 2010). The two runs differ on the location of the bifurcation point with respect to a steady bar. The second model application was meant to simulate the hypothetical implementation of a longitudinal training wall on a real river presenting some similarity with the upscaled case. This river is the Alpine Rhine River (Adami et al., 2016). The analysis focused on the effects of variable discharge, analysing the development of bars in the two bifurcating channels. Special attention was paid on high-flow conveyance of the bifurcating system with respect to the original channel. In both models, the longitudinal training wall was schematized as a thin longitudinal dam, assumed infinitely high, thus always separating the flow, even with the highest discharges.

Table 1 lists the morphodynamic characteristics of the systems reproduced in the laboratory and with the numerical model.

4. Laboratory investigation

4.1. Experimental set up

Following the method of Struiksma and Crosato (1989), who imposed an upstream asymmetric flow restriction, the formation of hybrid bars was obtained by placing a curved plate 2.5 m downstream of the inlet, obstructing 2/3 of the channel width (Fig. 2). The training wall consisted of a longitudinal steel plate, placed at a certain distance from

Table 1
Characteristics of laboratory experiments and numerical simulations in this study.

Parameters	Notation	Unit	Experiments*			Upscaled models	Alpine Rhine models**
			B, W1, W2	S1	S2		
Bar-formative discharge	$Q_{50\%}$	m^3/s	$4.5*10^{-3}$	$4*10^{-3}$	$5*10^{-3}$	220	1845
River width	B	m	0.4	0.4	0.4	30	85
Normal depth	h_0	m	0.044	0.044	0.043	3.343	4.665
Average velocity	v	m/s	0.25	0.23	0.29	2.19	4.65
Longitudinal bed slope	i	–	0.0025	0.0027	0.0026	0.0025	0.0029
Chézy coefficient	C	$m^{1/2}/s$	24	21	27.5	24	40
Froude number	Fr	–	0.383	0.348	0.448	0.383	0.688
Shields parameter	θ_0	–	0.135	0.194	0.068	0.135	0.137
Median sediment size	D_{50}	m	$0.5*10^{-3}$	$0.37*10^{-3}$	$1.0*10^{-3}$	$37*10^{-3}$	$60*10^{-3}$
Relative density of sediment	Δ	–	1.65	1.65	1.65	1.65	1.65
Observed bar mode	m_O	–					1
Observed bar length	L	m					1200–1700
Transport law	Meyer-Peter and Muller (1948)						
Width-to-depth ratio	B/h	–	9	9	9	9	18
Bar mode according to Eq. (1)	m	–	|0.78|	|0.99|	|0.59|	|0.78|	|0.95|
Theoretical hybrid bar wave-length	L_p	m	3.2	2.6	8	239	980
2D flow adaptation length	λ_w	m	1.31	0.98	1.66	98	380
2D water depth adaptation length	λ_s	m	0.23	0.28	0.17	17	98
2D interaction parameter	λ_s/λ_w	–	0.17	0.28	0.1	0.17	0.26

* Experiment scenarios B, W1, W2, S1 and S2 are explained in Table 3.
** Adami et al. (2016), upstream reach from km 0.00 to km 12.27.

the glass side wall, separating two parallel channels. The length of the steel plate was equal to the theoretical longitudinal wave-length of the bars (Table 1). Two starting locations of the training wall with respect to the first steady bar were considered: one at the upstream part of the bar and the other one at the next pool. The two locations were selected after having obtained an equilibrium bed configuration presenting clear fully-formed hybrid alternate bars. Fig. 2 shows the configuration corresponding to B_e:B_n = 1:3 when the ecological channel is 10 cm wide and the navigation channel 30 cm.

Both water and sediment were recirculated. The sediment characteristics are summarized in Table 2. The use of sands with different grain sizes allowed studying cases differing in sediment transport mechanism (degree of suspension) and transverse bed slope alteration of sediment transport direction. The latter was expected to be smaller for sediment having smaller size (S1) and larger for larger sediment sizes (S2). The experimental tests S1 and S2 (sensitivity analysis) were carried out using the same width ratio as the base-case scenario (Table 3), B_e:B_n = 1:3. For these tests, the upstream asymmetric flow restriction leading to the formation of hybrid alternate bars was obtained by placing a small transverse steel plate instead of a curved plate. The total number of performed laboratory tests is 13, see Table 3.

Table 2
Sediment characteristics used in the sensitivity analysis.

Characteristic diameter	Base-case (mm)	S1 (mm)	S2 (mm)
D_{15}	0.43	0.25	0.30
D_{50}	0.50	0.37	1.00
D_{65}	0.56	0.44	1.26
D_{90}	0.70	0.65	1.48

4.2. Data collection and data processing

Bed level and water level were recorded by 5 laser devices three times a day. Since lasers can penetrate water, the measurements were carried out during the experiment without drying up the channel. One laser device measured the water level and the other ones measured the bed level at four locations in transverse direction.

Due to the presence of relatively large dunes and ripples, the rough bed level data were filtered to clean out the bar signal. The filter used is

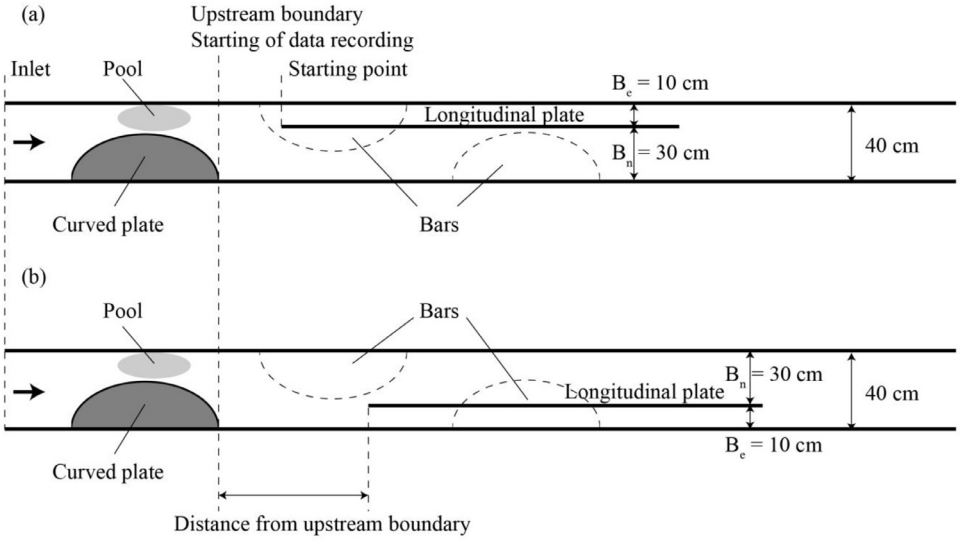

Fig. 2. Flume schematization (not to scale) with curved plate and longitudinal training wall represented by a longitudinal steel plate for B_e:B_n = 1:3 (base-case scenario). (a) Longitudinal plate starts at the upstream part of the first steady bar. (b) Longitudinal plate starts at the next pool.

Table 3
Experimental tests carried out in this study.

N^0	Scenarios	Notation in graph	Location with respect to a bar	Width ratio	Upstream constriction
1	Base case	B	Reference case	No training wall	Curved plate
2			Upstream	B_e:B_n = 1:3	
3			Pool		
4	Width 1	W1	Upstream	B_e:B_n = 1:5	
5			Pool		
6	Width 2	W2	Upstream	B_e:B_n = 1:1	
7			Pool		
8	Sensitivity 1	S1	Reference case	No training wall	Transverse plate
9			Upstream	B_e:B_n = 1:3	
10			Pool		
11	Sensitivity 2	S2	Reference case	No training wall	Transverse plate
12			Upstream	B_e:B_n = 1:3	
13			Pool		

based on the Matlab software ProcessV3 and optimized for bed forms having wavelengths larger than 1 m. The filtering procedure reduced the bar amplitude but allowed recognizing the bar geometry (pool, bar top, upstream and downstream parts of a bar). Bed level data were used to derive the temporal evolution of the averaged difference in bed level between the two parallel channels:

$$\Delta Z = Z_e - Z_n \quad (6)$$

in which Z_e and Z_n are the bed level in the ecological and the navigation channels, respectively, averaged over the entire length of the training wall.

The velocity field was measured using a Particle Tracking Velocimetry (PTV).

4.3. Results of the base-case scenario

All the tests of the base-case scenario started with the same bed topography (reference bed topography), presenting clear alternate bars, which was obtained after 10 days of morphological developments (Figs. 3 and 4(a)). The flow characteristics after 10 days are summarized in Table 1 and the characteristics of the sediment used are given in Table 2 (base-case scenario). The first two bars were steady with a wave length of about 3.2 m, while the remaining bars were shorter and migrating. The two bifurcation points were located 0.8 m and 1.8 m from the upstream boundary, respectively. In the first case the longitudinal steel plate started in the upstream part of the first steady bar. In the second case the longitudinal plate started in the pool. In both cases the "ecological channel" had a width of 10 cm and the "navigation channel" of 30 cm (Fig. 2).

The final configuration of the channel system at the end of the investigations is shown in Fig. 4. The temporal evolution of (averaged) bed topography (Fig. 5) shows progressive aggradation of the ecological channel and progressive degradation of the navigation channel if the longitudinal plate started in the upstream part of the bar (red line). After 10 days, the difference in averaged bed elevation between the two channels was $\Delta Z = 1.44$ cm, and this difference arose mainly due to sediment deposition in the ecological channel. The flow velocity in the ecological channel became gradually smaller than in the navigation channel. Fig. 6(a) shows the transverse velocity field after 10 days, at the end of this experimental test.

The ecological channel became increasingly deeper and the navigation channel shallower if the longitudinal plate started in the pool (Fig. 5, blue line). After 10 days, the difference in averaged bed elevation between the two channels was $\Delta Z = -2.6$ cm, which was mainly due to ecological channel bed erosion. The flow velocity in the ecological channel became progressively higher than in the navigation channel. Fig. 6(b) shows the transverse velocity field after 10 days, at the end of this experimental test.

4.4. Results of relative width variation

Changing the width of the parallel channels did not change the trends observed in the base-case scenario. If the longitudinal plate started in the upstream part of the bar the ecological channel silted up and the navigation channel became deeper. The opposite occurred if the longitudinal plate started in the pool. This means that the starting point of the longitudinal plate with respect to a steady bar influences the morphological process of the system more than the width distribution between the two channels. The latter was found to mainly influence the intensity and the speed of the process: the smaller the width ratio was, the faster the morphological evolution was. Fig. 7 shows the temporal evolution of the difference in bed elevation between the two channels for all cases. After 10 days, if the longitudinal plate started in the upstream part of the bar, the difference in bed elevation, ΔZ, was 2 cm for B_e:B_n = 1:5 (case W1); 1.46 cm for B_e:B_n = 1:3 (base case B) and 0.93 cm for B_e:B_n = 1:1 (case W2). On the contrary, when the longitudinal plate started in the pool, the results were −3.13 cm, −2.6 cm and −2.02 cm, respectively. These results suggest that the largest width ratio (channels having the same width), leading to the smallest difference in bed elevation between the two channels, may offer the best configuration in term of long-term morphology.

4.5. Sensitivity analysis

The sensitivity analysis was meant to qualitatively study the effects of varying sediment on the morphological trends of the system. This was done based on the initial trends, without reaching morphodynamic equilibrium. For this, the duration of the sensitivity-analysis tests was shorter: 3 days for each run. The longitudinal plate was placed 10 cm from the right side of the flume (B_e:B_n = 1:3). Each run started with a flat bed. The forcing offered by a small transverse plate assured that the hybrid bars always formed at the same location (Duró et al, 2015). The characteristics of the physical parameters are listed in Table 1. The

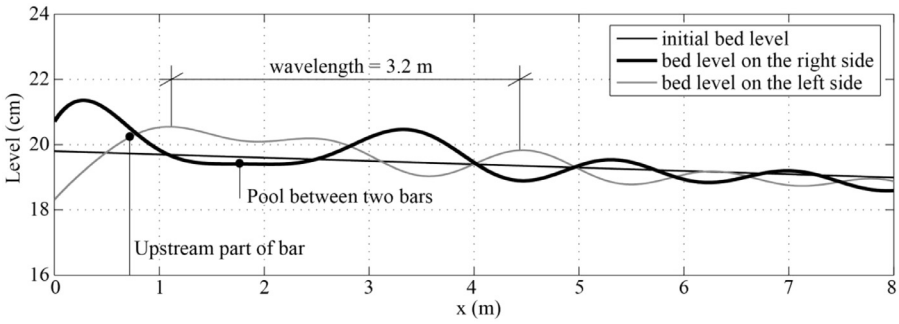

Fig. 3. Longitudinal bed level profiles showing hybrid alternate bars in the first 4 m after 10 days in the reference layout of the base-case scenario: filtered data.

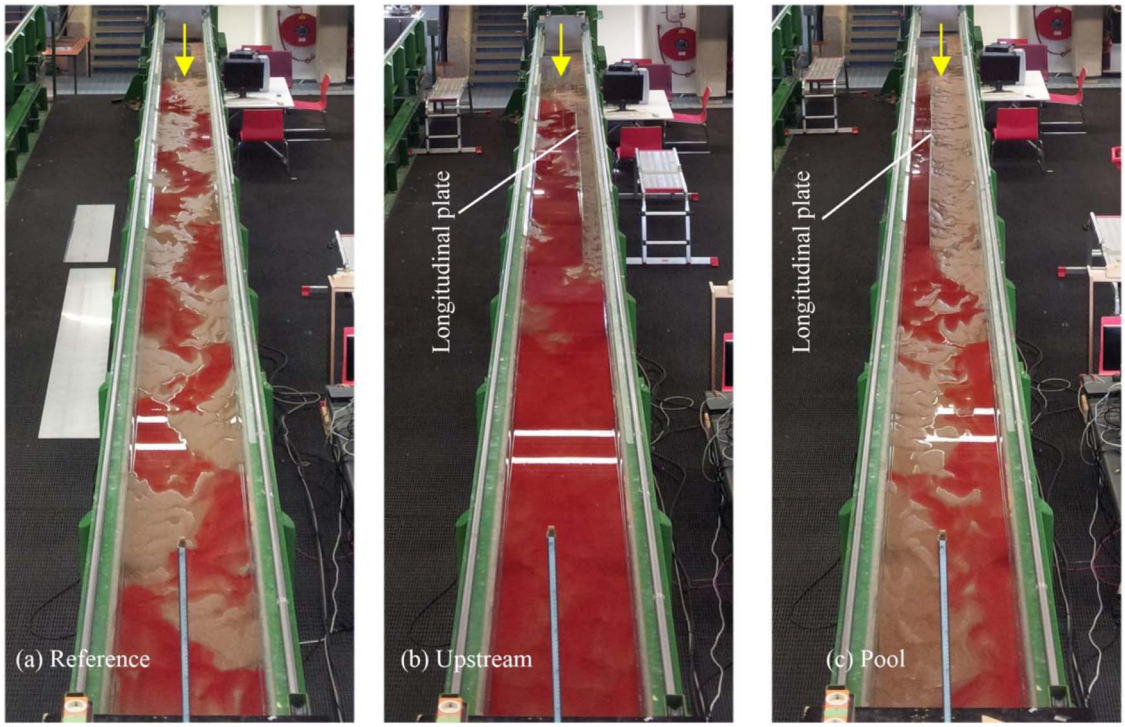

Fig. 4. Bed configuration of the base-case scenario at the end of the experiment after draining most of the water. (a) Hybrid and free alternate bars in the reference run without longitudinal plate. (b) Longitudinal plate starting in the upstream part of a steady bar: bed aggradation in the ecological channel and navigation channel deepening. (c) Longitudinal plate starting in a pool between two bars: bed aggradation in the navigation channel and ecological channel deepening. The yellow arrow indicates the flow direction. The blue line at the end of the flume is a ruler. The white crossing lines are the reflection of the neon light at the celling. (For interpretation of the references to color in this figure legend, the reader is referred to the web version of this article.)

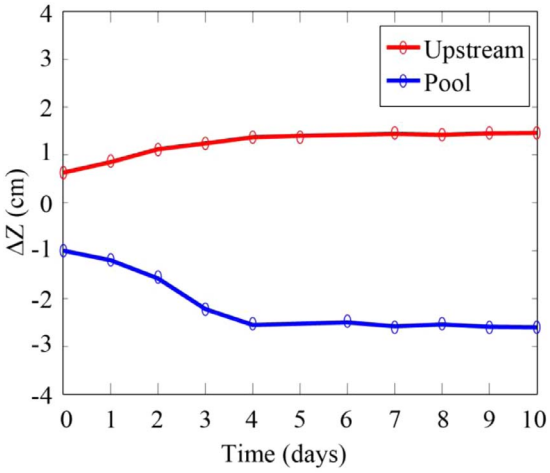

Fig. 5. Temporal evolution of the difference in bed elevation between the two parallel channels in the base-case scenario. "Upstream" refers to the case in which the longitudinal plate started in the upstream part of the first steady bar (red line). "Pool" refers to the case in which the plate started in the pool (blue line). (For interpretation of the references to color in this figure legend, the reader is referred to the web version of this article.)

characteristics of the sediment are listed in Table 2: S1 corresponds to the finer sand and S2 to the coarser one.

4.5.1. Results with finer sediment: test S1

In the reference scenario without longitudinal plate, hybrid alternate bars with a wavelength of 2.5 m and amplitude of 1 cm became well recognizable after 3 days (Fig. 8). In the subsequent tests, the longitudinal plate started either in the upstream part of the second bar or in the pool between the second and the third bar, 3.8 m and 5.0 m from the upstream boundary, respectively.

Fig. 9 shows the evolution of the difference in averaged bed elevation between the two channels (case S1 is represented by continuous lines).

When the longitudinal plate started in the pool, the ecological channel became progressively deeper than the main channel and the flow velocity in the ecological channel gradually became larger than in the navigation channel, confirming the results of the base case.

The ecological channel became slightly deeper and slightly conveyed more discharge also in the other test with the longitudinal plate starting in the upstream part of the bar. However, the results in this case might not be correct due to some discharge oscillations which were recognized only afterwards, when the experiment was finished already. In any case this result requires further checks.

4.5.2. Results with coarser sediment: test S2

In the reference scenario without a longitudinal wall, hybrid alternate bars with a wave length of 8 m were fully formed after 3 days. The long wavelength made the experiment particularly difficult, because the bars had also a rather small amplitude and this made it impossible to select a clear pool location. For the case of the plate starting in the upstream part of a bar, the starting point was placed at a distance of 4.4 m from the upstream boundary. Another starting location was investigated, this time close to the first bar top, at a distance of 6.7 m from the upstream boundary (Fig. 10).

The results are shown in Fig. 9 (dotted lines). When the training wall started in the upstream part of a bar, the ecological channel bed became gradually higher than the navigation channel bed. At the end of Day 3, the difference was 0.4 cm, mainly due to sediment deposition in the ecological channel. At the same time the flow velocity in the ecological channel became smaller than in the navigation channel. Although the duration of this test was only 72 h (3 days), this result shows a clear trend of deposition in the ecological channel, confirming the results of the base case.

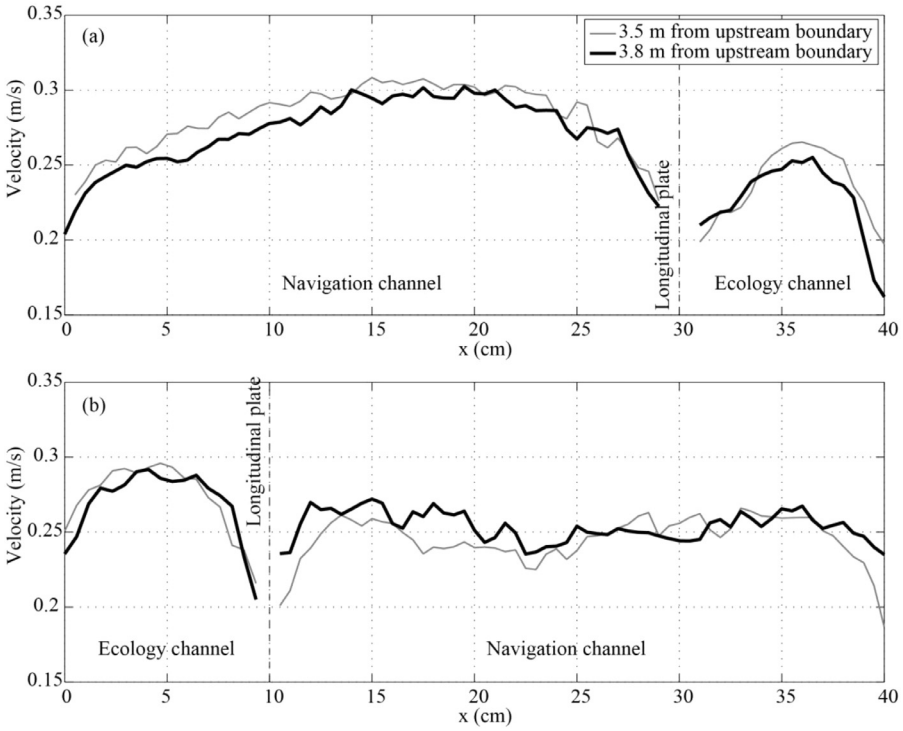

Fig. 6. Transverse velocity field in the base-case scenario after 10 days. (a) Longitudinal plate starting in the upstream part of the bar. (b) Longitudinal plate starting in the pool.

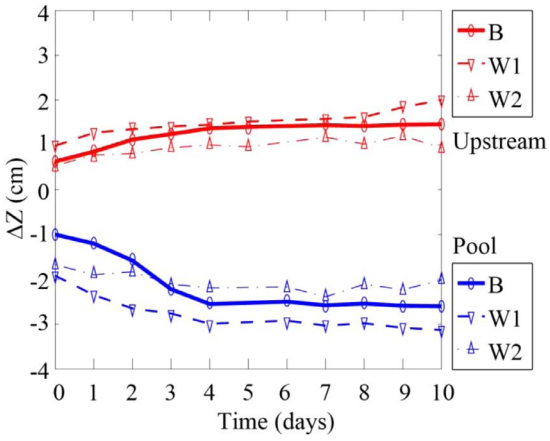

Fig. 7. Temporal evolution of the difference in bed elevation between the two parallel channels. "Upstream" refers to the case in which the longitudinal plate started in the upstream part of the first steady bar (red lines). "Pool" refers to the case in which the plate started in the pool (blue lines). The speed of the process is represented by the steepness of the curve. (For interpretation of the references to color in this figure legend, the reader is referred to the web version of this article.)

For the training wall starting near the bar top, the ecological channel slightly aggraded, whereas the flow velocity in the two channels remained almost the same. This could be a sign of ongoing aggradation or of a balance and should be further investigated.

5. Numerical investigation

5.1. Model description

This study constructed two-dimensional (2D) depth-averaged morphodynamic models using the Delft3D software. One model represented an upscaled version of the experimental flume and the other one a real river case. Delft3D has a finite difference scheme to solve the three-dimensional Reynolds equations for incompressible fluid under shallow water approximation and includes a morphodynamic module to account for sediment transport and bed level changes (Lesser et al., 2004). The two models were based on the depth-averaged version of the basic equations, which was demonstrated to be sufficient to reproduce bars with sufficient accuracy (e.g. Defina, 2003; Schuurman et al., 2013; Duró et al., 2015; Singh et al., 2017). The influence of the spiral flow in curved reaches was accounted for according to the formulation of Struiksma et al., (1985). The roughness was represented by a constant

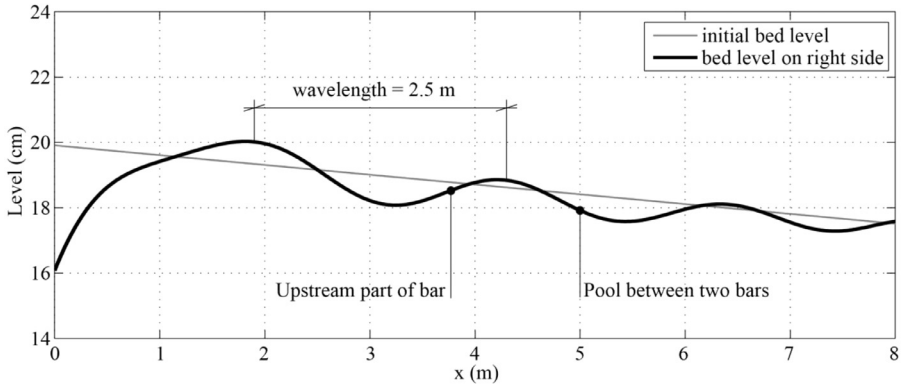

Fig. 8. Longitudinal bed level profile showing hybrid alternate bars after 72 h with finer sediment (test S1): filtered data.

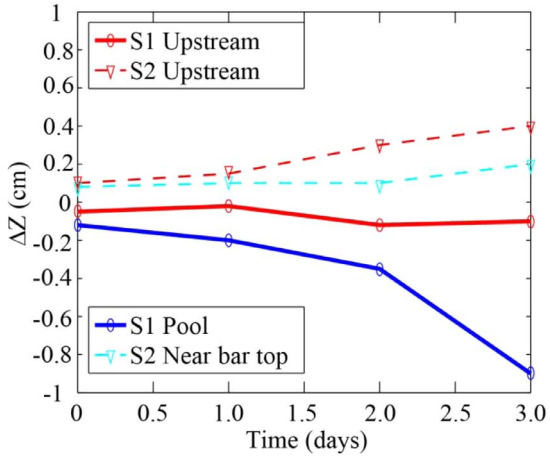

Fig. 9. Temporal evolutions of the difference in bed elevation between the two parallel channels (sensitivity analysis). Continuous lines refer to sediment S1 and dash lines to sediment S2. Red lines refer to the cases in which the longitudinal plate started in the upstream part of the bar. The blue line represents the case in which the longitudinal plate started in the pool and the light blue line near the bar top. (For interpretation of the references to color in this figure legend, the reader is referred to the web version of this article.)

Chézy coefficient (values in Table 1) and the bed-load transport rate was computed by means of the Meyer–Peter and Müller (1984) (MPM) formula, valid for sand and gravel-bed rivers. The effects of transverse bed slope on sediment transport direction were taken into account according to Bagnold's (1966) formulation (default in Delft3D). Not considering these effects would result in an un-realistic unstable model (Mosselman and Le, 2016).

The hydrodynamic boundary conditions of the models consisted of downstream water level and upstream discharge. In the upscaled model, these boundary conditions were constant values, whereas in the Alpine Rhine model they were variable, according to the discharge variations. The boundary conditions for the sediment component were defined by upstream balanced sediment transport, which prevented the bed level from changing at the boundary, and downstream free sediment transport condition, which may result in bed level changes. The lateral banks were fixed and treated as free-slip fixed boundaries.

The time step of the flow was 0.1 min to ensure numerical stability as evaluated by the Courant criterion for fluid advection. To fully reproduce the interaction between flow and sediment, the computations were carried out without any morphological acceleration. The longitudinal training wall was schematized as a thin, infinitely high and deep, dam. This ensured that the structure always divides the two channels. The length of the wall was equal to the bar wave length and obtained after completion of a reference run. A transverse groyne obstructing 2/3 of the width was placed at the right side wall at a certain distance from the upstream boundary to trigger hybrid bars. Table 4 shows the exact distance and the numerical parameters in both models.

Table 4
Values of variables and parameters used in the numerical simulations studying an upscaled version of the laboratory experiments.

Parameters	Notation	Unit	Upscale	Alpine Rhine
Length of computational domain	L	m	2250	4250
Rectangular grid size	$M \times N$	m	2.5 × 7.5	7.08 × 21.25
Time step	t	minutes	0.1	0.1
Simulation time	T	days	10	3*365
Location of forcing (transverse groyne)	–	m	375	510
Morphological factor	MF	–	1	1
Transport law	Meyer-Peter and Muller (1948)			

5.2. Upscaled-experiment model setup

This numerical simulation aimed at establishing whether a 2D morphodynamic model constructed using the Delft3D software provides reliable results when studying the effects of subdividing a straight river channel with alternate bars with a longitudinal training wall.

The hydraulic and morphology parameters in the upscaled version of the laboratory tests are presented in Table 1. The numerical parameters are summarized in Table 4.

The reference case, without longitudinal wall, started with a flat bed. A transverse groyne, located 375 m from the upstream inlet on the right side was used to assure the formation of the hybrid bars as in Duró et al. (2015), reproducing the effects of the curved plate placed in the flume. The results obtained after 10 days of morphological development are shown in Fig. 11. In this figure, the results are plotted from the transverse groyne to the end of the reach. The shape of the alternate bars qualitatively resembles the one obtained in the laboratory for the reference case (Fig. 3), with a long steady bar opposite to the groyne and smaller migrating bars more downstream. This means that the similarity based on longitudinal slope, Shield parameter, width-to-depth ratio, bar mode, interaction parameter (Table 1), does not result in quantitative geometric similarity, but only in qualitative geometric similarity.

In the same way as in the experiment, two locations for the starting point of the longitudinal wall were considered: one in the upstream part of the first steady bar and one in the pool opposite to it (Fig. 11). For each location, three different width ratios were considered: B_c:B_n = 1:5, 1:3 and 1:1. All upscaled-experiment scenarios (Table 5) started from the bed topography shown in Fig. 11. The computations simulated a period of 10 days.

5.3. Upscaled-experiment model results

In the base-case scenario (B runs), when the longitudinal training wall starts from the upstream part of a bar, the result shows that the

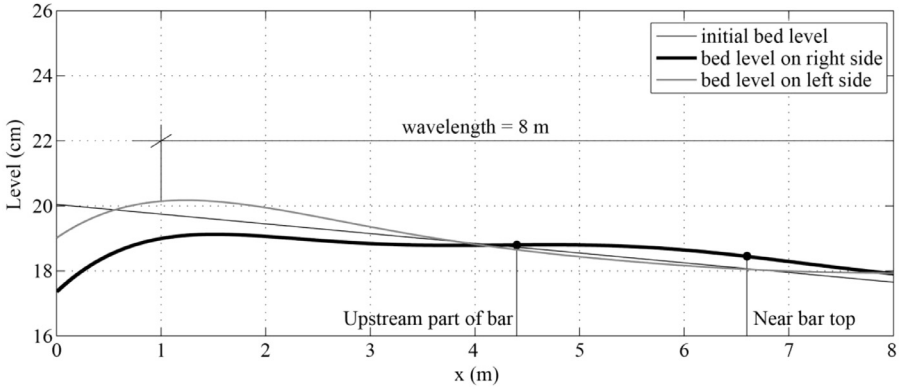

Fig. 10. Longitudinal bed level profiles showing hybrid alternate bars after 72 h with coarser sediment (test S2): filtered data.

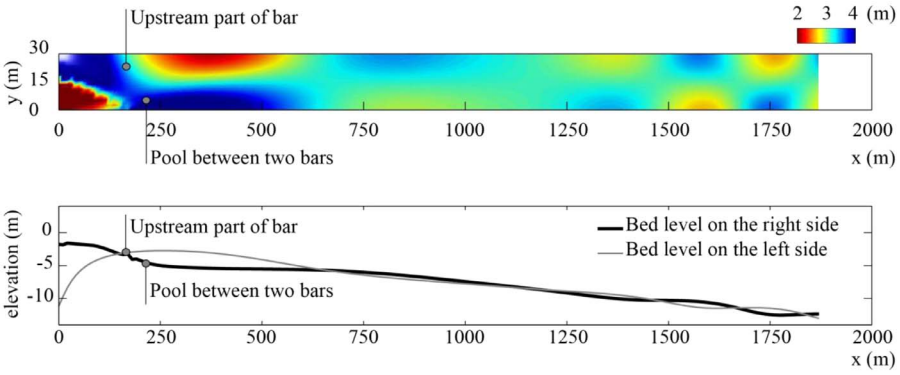

Fig. 11. Alternate bars in the reference case of the upscaled model and locations of the starting points of the longitudinal wall (grey dots). Upper panel: Water depth distribution. Lower panel: near-bank longitudinal bed level profiles.

smaller ecological channel silts up (Fig. 12(a)). The opposite occurs, when the training wall starts at a pool location (Fig. 12(b)).

The trends are the same also for different width ratios. If the training wall starts in the upstream part of the bar the ecological channel silts up. Instead, if the training wall starts in the pool between two bars the ecological channel deepens whereas the navigation channels aggrades. As in the experiments, also in the numerical simulations the width ratio influences the speed of the process (see Fig. 13) in the same way as in the experimental test (Fig. 7).

All the obtained numerical results are similar to the ones obtained in the laboratory, supporting the use of the numerical model to study a real river case with variable discharge.

5.4. Alpine Rhine model setup

This numerical investigation aimed at studying the effects of variable discharge in a real river case that is rather similar to the upscaled version of the system studied in the laboratory. The analysis focused on conveyance capacity and bar formation. The selected case study is the Upper Reach of the Alpine Rhine River described by Adami et al. (2016). The characteristics of the system are listed in Table 1. The numerical parameters are summarized in Table 4.

The hydrograph used in this model considered the three discharge levels indicated by Adami et al.: fully wet discharge Q_{FW} = 381 m^3/s, fully transporting discharge Q_{FT} = 829 m^3/s, and critical discharge for bar formation Q_{cr} = 1845 m^3/s. The duration of these discharges was derived from Fig. 2 in Adami et al. (2016) to roughly describe a typical year (Fig. 14).

The model schematized the river reach as straight, although the channel presents a slight curvature (Fig. 1). Since the model was not meant to reproduce each bar observed in the study reach, but to simulate the effects of subdividing the river channel with a longitudinal wall, a transverse groyne, located 500 m from the upstream boundary was placed at the right side to obtain hybrid bars, in the same way as in the upscaled-experiment model. For this the model was not calibrated, but validated in terms of bar mode and bar wave-length.

The reference case, without longitudinal wall, started with a flat bed. The bed topography obtained after 3 years is shown in Fig. 15. In this figure, the bed elevation is plotted from the transverse groyne to the end of the reach. The computed steady alternate bar configuration corresponds rather well to the observed one, considering that also the celerity of the observed bars in the real river reach is zero or close to zero. Moreover, the computed wave length of the alternate bars is 1500 m, which nicely falls within the observed range (Adami et al., 2016) (Fig. 1).

Two locations for the starting point of the longitudinal wall were considered: one in the upstream part of the first steady bar and one in the pool opposite to it. Only one width ratio was considered: B_e:B_n = 1:3. All the Alpine Rhine scenarios (Table 6) started from the bed topography shown in Fig. 15. Each computation simulated a period of 3 years.

5.5. Alpine Rhine model results

In general, based on the results obtained after 3 years, the morphological trends computed for the Alpine Rhine with variable discharge agree with the results of the laboratory tests and upscaled model. When the longitudinal training wall starts in the upstream part of a steady bar the smaller ecological channel silts up (Fig. 16). The opposite occurs when the training wall starts in a pool location (Fig. 17).

Fig. 16 shows that when the training wall starts in the upstream part of a bar, under high discharge, the ecological channel silts up but both channels remain open (Fig. 16(a)) whereas with low flow the ecological channel is completely closed and the navigation channel conveys the entire discharge (Fig. 16(b) and (c)). When all water flows in the navigation channel smaller and shorter bars are found compared to the reference case. Downstream of the training wall, the bars remain of the same type as in the reference case. In this scenario, the training wall helps to reduce the hinder of the bars in the navigation channel.

When the longitudinal training wall starts in the pool between two bars, with high discharge the ecological channel conveys almost all water but both channels remain open (Fig. 17(a)). With the smallest discharge the navigation channel closes and all water flows in the ecological channel (Fig. 17(b) and (c)). In this scenario the navigation channel is not functional at all at low water.

Fig. 18 shows the longitudinal profiles of water and bed levels in both the ecological and the navigation channel during the highest

Table 5
Overview of the upscaled-experiment simulations.

N^0	Scenarios	Notation in graph	Location with respect to a bar	Width ratio	Initial bed level	Description
1	Base case	B	Reference case	No training wall	Flat bed	B runs study the effects of starting location of the training wall
2			Upstream	B_1:B_2 = 1:3	Hybrid bars	
3			Pool			
4	Width 1	W1	Upstream	B_1:B_2 = 1:5		W runs study the effects of width ratio
5			Pool			
6	Width 2	W2	Upstream	B_1:B_2 = 1:1		
7			Pool			

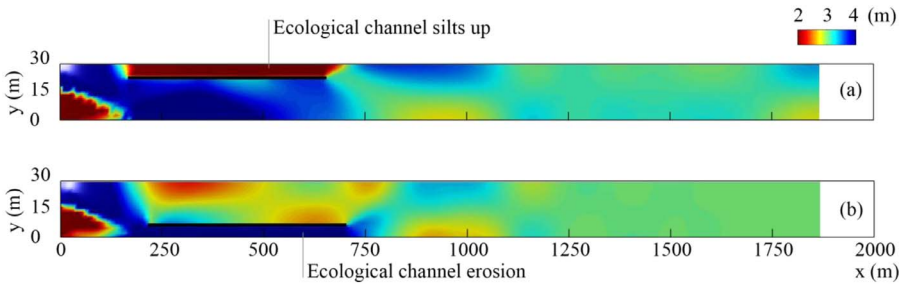

Fig. 12. Water depth distribution showing the morphological development in base-case scenario. (a) Longitudinal wall starting in the upstream part of a steady bar. (b) Longitudinal wall starting in the pool between two bars.

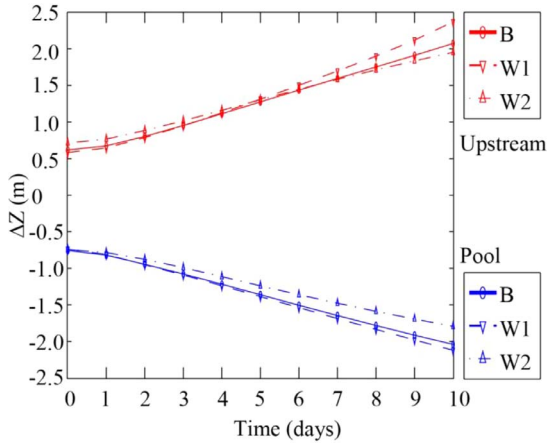

Fig. 13. Temporal evolution of the difference in bed elevation between the two parallel channels. Red lines represent the cases in which the training wall started in the upstream part of the bar and the blue lines the cases in which the training wall started in the pool. The speed of the process is represented by the steepness of the curve. (For interpretation of the references to color in this figure legend, the reader is referred to the web version of this article.)

discharge. These results show that the longitudinal training wall does not hamper the flood conveyance during high flows.

If the training wall starts in the upstream part of a bar, there is a 1.2 m drop of water level in the ecological channel (Fig. 18(a)) whereas in the navigation channel the water level is almost the same as in the reference case (Fig. 18(b)). At the downstream end of the training wall there is a slight increasing in water level compared to the reference case (10 cm). This could be the influence of the confluence where the parallel channels merge again.

If the training wall starts in the pool between two bars, the water level in the ecological channel drops by maximum 50 cm (Fig. 18(c)) and in the navigation channel by a maximum of 65 cm (Fig. 18(d)). However, near the downstream end of the training wall the water level rises up to 28 cm. In this scenario, the rise of water level due to the confluence appears more important.

The effects of using a constant Chézy coefficient might have resulted in overestimating the conveyance of the aggrading channel for which the roughness is most likely underestimated. At the same time, the conveyance of the deepening channel might be slightly underestimated.

6. Discussion

The experiments were carried out on straight channels, whereas real rivers present numerous curves. The point bars at the inner side of bends may act as steady alternate bars in affecting the distribution of water and sediment between the two parallel channels, but river bends also result in spiral flow formation and this might alter the direction of sediment transport. For this, the presence of river bends might affect the results of this study. We therefore recommend studying the effects of a longitudinal training wall in a meandering channel.

The numerical results were obtained assuming constant hydraulic resistance, represented by Chézy coefficient. However, channel deepening might result in smaller hydraulic resistance (larger Chézy coefficient) whereas the channel becoming shallower might result in higher hydraulic resistance (smaller Chézy coefficient). Small-scale (sub-grid) bedform formation would influence the Chézy coefficient as well. These effects are not taken into account in the computations. Moreover, due to the alternation of high and low discharges, vegetation might colonize the shallow channel during low flow and drastically increase its bed roughness during high flow. This can reduce the flood conveyance of the parallel channel system.

The work considered gravel-bed rivers, since the laboratory experiments, even though sand was used, represented a river with gravel bed (the characteristics of the laboratory experiments and of the upscaled river are shown in Table 1). The subsequent real-river case was again a gravel-bed river with alternate bars. This means that the results are strictly valid only for gravel-bed rivers and their applicability on sand-bed systems requires further investigation.

The strategy we propose to train rivers by creating a navigation and ecological channel with a longitudinal wall presents advantages and disadvantages. We have shown that the bifurcation created with a longitudinal wall results in an unstable system in which one of the two channels inevitably becomes shallower, ideally the ecological channel. This channel closes completely only if the discharge is constant; with variable discharge, it becomes dry at low flows only. This would be an advantage for navigation, because the flow then concentrates in the other channel, increasing the low-flow water depth. The temporary, seasonal, closure of the ecological channel, however, might be a disadvantage for the riverine ecology and this should be further investigated by experts in this field.

In rivers with hybrid alternate bars (rather common in real cases), the results show also that if the training wall starts in the upstream part of a steady bar the smaller ecological channel experiences sediment

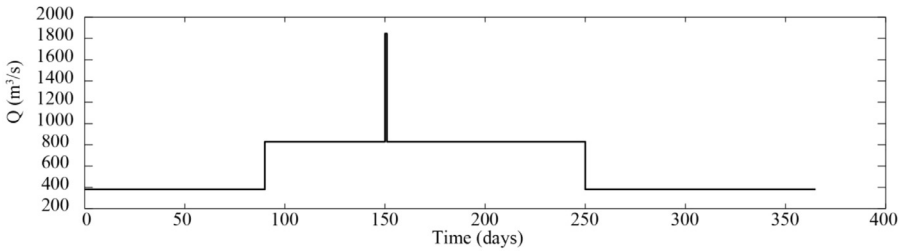

Fig. 14. Hydrograph for a typical year used in Alpine Rhine model.

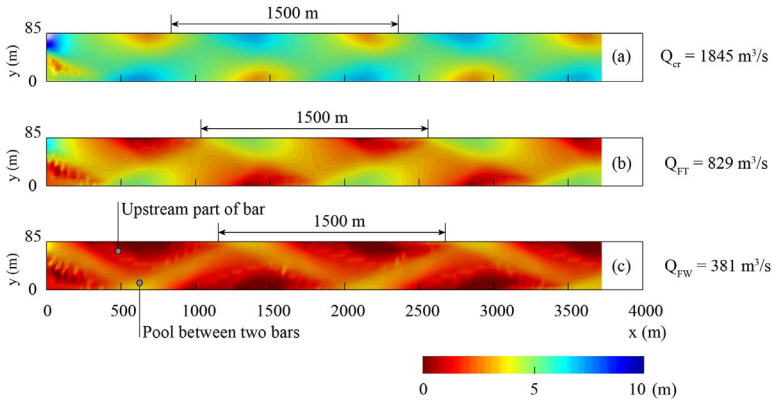

Fig. 15. Alpine Rhine model results: water depth distributions showing alternate bars in the reference scenario, without longitudinal wall, at the end of the each discharge in the third year. The gray dots in (c) indicate the location of the starting points of the longitudinal wall. (For interpretation of the references to color in this figure legend, the reader is referred to the web version of this article.)

Table 6
Overview of the Alpine Rhine simulations.

N⁰	Scenarios	Notation in graph	Location with respect to a bar	Width ratio	Initial bed level	Description
1	Variable discharge	V	Reference case	No training wall	Flat bed	V runs study the effects of variable discharge
2			Upstream	B_e:B_n = 1:3	Hybrid bars	
3			Pool			

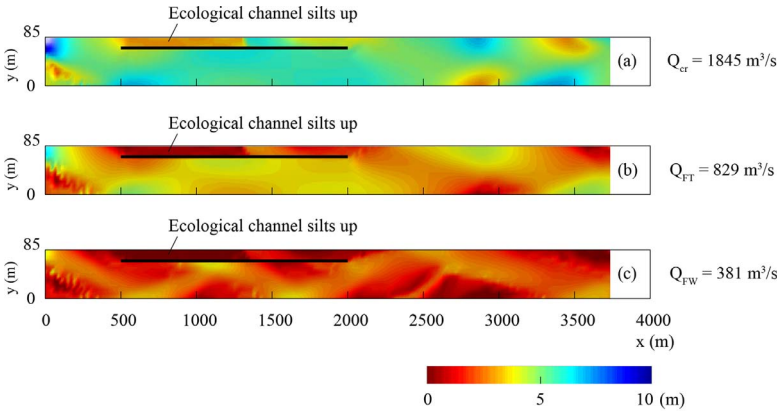

Fig. 16. Water depth distribution showing the morphological developments at the end of the each discharge in the third year if the longitudinal wall started in the upstream part of a steady bar.

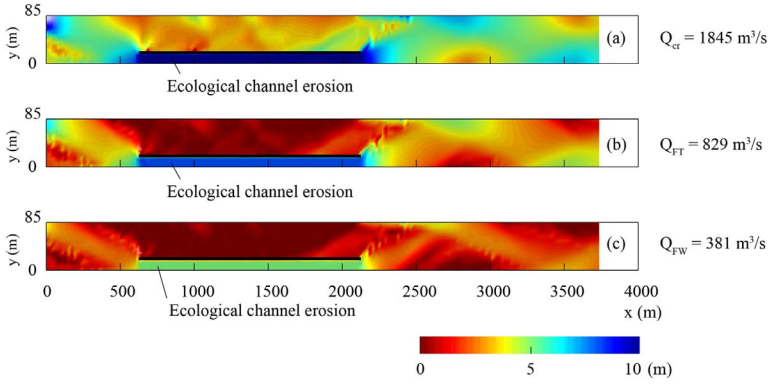

Fig. 17. Water depth distribution showing the morphological developments at the end of the each discharge in the third year if the longitudinal wall started in the pool between two bars.

deposition and the navigation channel becomes deeper. In this case, the flood conveyance of the river is not reduced, which means that the construction of the longitudinal wall does not increase flood risk in the area adjacent to the river. The opposite happens if the training wall starts in the pool between two bars: the navigation channel silts up and the flood conveyance of the river reduces. These results show the importance of well designing the starting point of the longitudinal wall.

The time scales involved in the processes plays an important role too. If the morphological development is slow, it could be possible to maintain both channels open by, for instance, dredging and dumping the deposited sediment from one channel to the other. This means that the applicability of the proposed technique requires more research.

7. Conclusions

We studied the possibility of subdividing a river channel in one relatively narrow “ecological channel” and one “navigation channel” by means of a longitudinal training wall in the laboratory and by means of

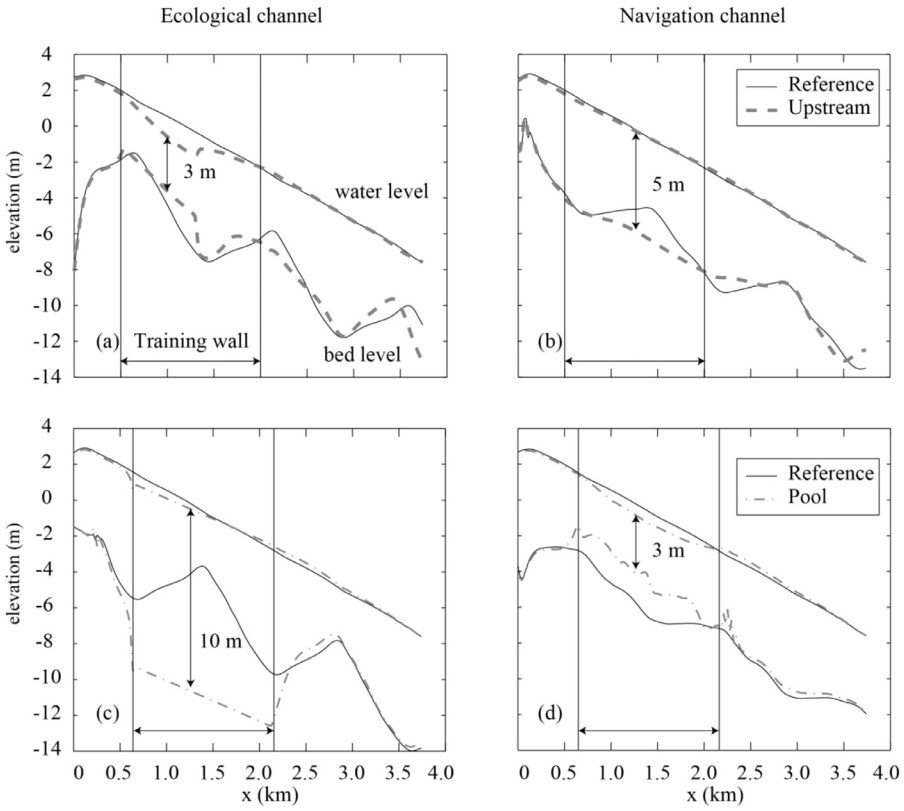

Fig. 18. Longitudinal profiles along the centre line of the ecological and navigation channels during high flow (Q_{cr} = 1845 m^3/s). In (a) and (b) the longitudinal wall started in the upstream part of a steady bar (upstream), whereas in (c) and (d) the longitudinal wall started in the pool between two bars (pool). "Reference" refers to the case without longitudinal wall.

numerical simulations. We considered channels characterized by the presence of steady alternate bars, which are common morphological features hindering river navigation.

The laboratory experiments show that subdividing a channel presenting steady or slowly migrating alternate bars with a longitudinal training wall might lead to an unstable system, in which one of the two parallel channels tends to silt up. The results show that the starting point of the longitudinal wall with respect to a bar plays an important role for the morphological evolution of the two channels. When the training wall starts at a location in the upstream part of a bar, the narrower ecological channel silts up. Instead, when the training wall starts in the pool area between two subsequent bars, the same channel deepens and the navigation channel silts up. Changing the widths of the channels did not change the trends observed in the base-case scenario. The most stable system is obtained if the longitudinal wall subdivides the river in two equally-wide parallel channels. Changing sediment did not alter the observed trends too, with the exception of test S1 (finer sediment) for which some problems encountered during the experiment did not allow to draw any conclusions for the case starting in the upstream part of a bar. One experimental test (S2: coarser sediment) indicates that a stable system might be obtained if the training wall starts near a bar top, but this might not be true with a variable discharge regime and should be further investigated.

These observations were reproduced numerically in an upscaled version of the laboratory experiments, supporting the use of a 2D model based on the numerical code Delft3D to investigate this type of systems on a real river case.

The subsequent use of the code to study the effects of placing a longitudinal training wall in the Upper Reach of the Alpine Rhine River described by Adami et al. (2016) confirms the observed trends and shows that a variable discharge regime does not change the observed trends.

The conveyance of the channel was studied by comparing the water levels in presence of longitudinal wall with those in a reference scenario without wall. The results show that the longitudinal training wall affects high-flow water levels only slightly if it starts in the upstream part of a bar. In this case, a small increase of water level is observed near the downstream end of the longitudinal wall. However, if the training wall starts in the pool between two bars the raise of high-flow level near the end of the longitudinal wall is not negligible, even if limited.

Acknowledgments

This work is sponsored by Vietnam International Education Development (VIED). The authors wish to thank Floortje Roelvink, Anouk Lako and the technical staff of the Environmental Fluid Mechanics Laboratory of Delft University of Technology.

Supplementary materials

Supplementary material associated with this article can be found, in the online version, at doi:10.1016/j.advwatres.2018.01.007.

References

Adami, L., Bertoldi, W., Zolezzi, G., 2016. Multidecadal dynamics of alternate bars in the Alpine Rhine River. Water Resour. Res. 52. http://dx.doi.org/10.1002/2015WR018228.

Army Corps of Engineers, 2011. Upper Mississippi River Navigation Charts: Minneapolis, MN to Cairo, IL Upper Mississippi River Miles 866 to 0. Publisher: Defense Dept., Army Corps of Engineers, Mississippi Valley Division, Minnesota and St. Croix Rivers, pp. 286 ISBN: 9780160934377.

Bagnold, R.A., 1966. An Approach to the Sediment Transport Problem from General Physics. U. S. Govt. Print. Off, Washington.

Bertoldi, W., Zanoni, L., Miori, S., Repetto, R., Tubino, M., 2009. Interaction between migrating bars and bifurcations in gravel bed rivers. Water Resour. Res. 45, W06418. http://dx.doi.org/10.1029/2008WR007086.

British Marine Federation and Environment Agency, 2013. Cruising Guide to the River Thames and Connecting Waterways 2013-2014. Environment Agency, LIT 6689. www.gov.uk/government/publications/river-thames-and-connecting-waterways-cruising-guide.

Callander, R.A., 1969. Instability and river channels. J. Fluid Mech. 36 (3), 465–480.

Chavarrías, V., Blom, A., Orrú, C., Viparelli, E., 2013. Laboratory experiment of a mixed-

sediment Gilbert delta under varying base level. In: Extended abstr. RCEM 2013. Spain. Santander, pp. 114.
Crosato, A., Mosselman, E., 2009. Simple physics-based predictor for the number of river bars and the transition between meandering and braiding. Water Resour. Res. 45, W03424. http://dx.doi.org/10.1029/2008WR007242.
Defina, A., 2003. Numerical experiments on bar growth. Water Resour. Res. 39, 1–12. http://dx.doi.org/10.1029/2002WR001455.
De Vriend, H.J., 2015. The long-term response of rivers to engineering works and climate change. Proc. Instit. Civil Eng. Water Manage. 168 (3), 139–144. http://dx.doi.org/10.1680/cien.14.00068.
Duró, G., Crosato, A., Tassi, P., 2015. Numerical study on river bar response to spatial variations of channel width. Adv. Water Resour. 93, 21–38. http://dx.doi.org/10.1016/j.advwatres.2015.10.003.
Elbe Promotion Centre website: www.elbpro.com/en/elbe/waterway-in-a-cultural-landscape.html.
Engelund, F., 1970. Instability of erodible beds. J. Fluid Mech. 42 (3), 225–244.
Flokstra, C., 1985. De Invloed Van Knooppuntsrelaties Op De Bodemligging Bij Splitsingspunten. Waterloopkundig Laboratorium (WL | Delft Hydraulics) (in Dutch) Report r2166.
Fredsøe, J., 1978. Meandering and braiding of rivers. J. Fluid Mech. 84 (4), 609–624.
Frings, R.M., Döring, R., Beckhausen, C., Schüttrumpf, H., Vollmer, S., 2014. Fluvial sediment budget of a modern, restrained river: The lower reach of the Rhine in Germany. Catena 122, 91–102. http://dx.doi.org/10.1016/j.catena.2014.06.007.
Hansen, E., 1967. On the Formation of Meanders as a Stability Problem. Coastal Engineering, Laboratory, Technical Univ. Denmark, Basis Research, pp. 9 Progress Report 13.
Havinga, H., Taal, M., Smedes, R., 2006. Recent Training of the Lower Rhine River to Increase Inland Water Transport potentials: A mix of Permanent and Recurrent measures, River Flow 2006. In: Leal, Ferreira, Alves, Cardoso (Eds.), Taylor & Francis Group, London ISBN 0-415-40815-6.
Jansen, P.P., van Bendegom, L., van den Berg, J., de Vries, M., Zanen, A., 1979. Principles Of River Engineering: The Non-Tidal Alluvial River. Pitman London Facsimile edition published in 1994 by Delft: Delftse U.M.ISBN 90-6562-146-6.
Kleinhans, M.G., van Dijk, W.M., van de Lageweg, W.I., Hoendervoogt, R., Markies, H., Schuurman, F., 2010. From Nature to Lab: Scaling Self-Formed Meandering and Braided rivers, River Flow 2010. In: Aberle, Dittrich, Koll, Geisenhainer (Eds.), © 2010 Bundesanstalt für Wasserbau ISBN 978-3-939230-00-7.
Lesser, G.R., Roelvink, J.A., van Kester, J.A.T.M., Stelling, G., 2004. Development and validation of a three-dimensional morphological model. J. Coastal Eng. 51, 883–915.
Mekong River Commission, 2016. Strategic Plan 2016 - 2020. http://www.mrcmekong.org/assets/Publications/strategies-workprog/MRC-Stratigic-Plan-2016-2020.pdf.
Meyer-Peter, E., Müller, R., 1948. Formulas for bed-load transport. In: Proc., 2nd Meeting. Stockholm, Sweden. IAHR, pp. 3964.
Mosselman, E., Le, T.B., 2016. Five common mistakes in fluvial morphodynamic modeling. Adv. Water Resour. 93, 15–20. http://dx.doi.org/10.1016/j.advwatres.2015.07.025.
Mosselman, E., Kerssens, P., van der Knaap, F., Schwanenberg, D., Sloff, C.J., 2004. Sustainable River Fairway Maintenance and Improvement - Literature Survey. WL | Delft Hydraulics Technical Report Q3757.00.
NEPAD Agency, 2013. www.nepad.org/content/construction-navigational-line-between-lake-victoria-and-mediterranean-sea.
Parker, G., 1976. On the cause and characteristic scales of meandering and braiding in rivers. J. Fluid Mech. 76 (3), 457–479.
Redolfi, M., Zolezzi, G., Tubino, M., 2016. Free instability of channel bifurcations and morphodynamic influence. J. Fluid Mech. 799, 476–504. http://dx.doi.org/10.1017/jfm.2016.389.
Rijke, J., van Herk, S., Zevenbergen, C., Ashley, R., 2012. Room for the River: delivering integrated river basin management in the Netherlands. Int. J. River Basin Manage. 10 (4), 369–382. http://dx.doi.org/10.1080/15715124.2012.739173.
Scerri, F., Lescoulier, C., Boudong, C., Hémain, C., et al., 2015. 2D Modelling of the Rhone River Between Arles and the Sea in the Frame of the Flood Prevention Plan. In: Gourbesville, P. (Ed.), Advances in Hydroinformatics. Springer Water, pp. 253–273. http://dx.doi.org/10.1007/978-981-287-615-7_18.
Schoor, M.M., Wolfert, H.P., Maas, G.J., Middelkoop, H., Lambeek, J.J.P., 1999. Potential for floodplain rehabilitation based on historical maps and present-day processes along the River Rhine, the Netherlands. In: Marriott, S.B., Alexander, J. (Eds.), Floodplains: Interdisciplinary Approaches, Geological Society 163. Special Pub., London, pp. 123–137.
Schuurman, F., Marra, W.A., Kleinhans, M.G., 2013. Physics-based modeling of large braided sand-bed rivers: Bar pattern formation, dynamics, and sensitivity. J. Geophys. Res. Earth Surf. 118 (4), 2509–2527. http://dx.doi.org/10.1002/2013JF002896.
Sieben, J., 2009. Sediment management in the Dutch Rhine branches. Int. J. River Basin Manage. 7 (1), 43–53. http://dx.doi.org/10.1080/15715124.2009.9635369.
Singh, U., Crosato, A., Giri, S., Hicks, M., 2017. Sediment heterogeneity and discharge variability in the morphodynamic modelling of gravel-bed braided rivers. Adv. Water Resour. http://dx.doi.org/10.1016/j.advwatres.2017.02.005.
Sloff, K., Mosselman, E., 2012. Bifurcation modelling in a meandering ravel-sand bed river. Earth Surf. Process. Landf. 37, 1556–1566.
Spinewine, B., Zech, Y., 2008. An ex-post analysis of the German Upper Rhine: data gathering and numerical modelling of morphological changes in the 19th century. J. of Flood Risk Manage. 1, 57–68. http://dx.doi.org/10.1111/j.1753-318X.2008.00007.x.
Struiksma, N., Crosato, A., 1989. Analysis of a 2 D bed topography model for Rivers. In: Ikeda, S., Parker, G. (Eds.), River Meandering 12. Water Resources Monograph, pp. 153–180 ISBN 0-87590-316-9.
Struiksma, N., Olesen, K.W., Flokstra, C., de Vriend, H.J., 1985. Bed deformation in curved alluvial channels. J. Hydr. Res. 23 (1), 57–79.
Talmon, A.M., Struiksma, N., van Mierlo, M.C.L.M., 1995. Laboratory measurements of the direction of sediment transport on transverse alluvial-bed slopes. J. Hydr. Res. 33 (4), 495–517.
Tubino, M., 1991. Growth of alternate bars in unsteady flow. Water Resour. Res. 27 (1), 37–52.
Tubino, M., Seminara, G., 1990. Free-forced interactions in developing meanders and suppression of free bars. J. Fluid Mech. 214, 131–159.
Tubino, M., Repetto, R., Zolezzi, G., 1999. Free bars in rivers. J. Hydr. Res. 37 (6), 759–775.
van Vuren, S., Paarlberg, A., Havinga, H., 2015. The aftermath of “Room for the River” and restoration works: Coping with excessive maintenance dredging. J. Hydro-Environ. Res. 9 (2), 172–186. http://dx.doi.org/10.1016/j.jher.2015.02.001.
Villada Arroyave, J.A., Crosato, A., 2010. Effects of river floodplain lowering and vegetation cover. Proc. of I.C.E. Water Manage. 163 (9), 457–467. http://dx.doi.org/10.1680/wama.900023.
Visser, P.J., Havinga, H., ten Brinke, W.B.M., 1999. Hoe houden we de rivier bevaarbaar? Land + Water 39 (9), 24–27 (in Dutch).
Wang, Z.B., Fokkink, R.J., de Vries, M., Langerak, A., 1995. Stability of river bifurcations in 1D morphodynamic models. J. Hydr. Res. 33 (6), 739–750.
Zolezzi, G., Seminara, G., 2001. Downstream and upstream influence in river meandering. Part 1. General theory and application to overdeepening. J. Fluid Mech. 438, 183–211.